06,15

Dielectric properties and kinetics of induced phase transition in ceramic compounds $16BiScO_3-42PbTiO_3-42PbMg_{1/3}Nb_{2/3}O_3$

© L.S. Kamzina, V.G. Zalesskii

Ioffe Institute,
St. Petersburg, Russia

E-mail: ASKam@mail.ioffe.ru

Received February 2, 2025
Revised February 3, 2025
Accepted February 3, 2025

The relationship between the depolarization temperatures T_d and the morphotropic phase transition $T_{\text{F-R}}$ in the relaxor ceramics $16BiScO_3-42PbTiO_3-42PbMg_{1/3}Nb_{2/3}O_3$, as well as the kinetics of nucleation of ordered ferroelectric phases in an electric field applied below the morphotropic phase transition temperature, were studied. The coincidence of these temperatures was found, which is associated with a one-stage transition of the polarized sample to the relaxor phase. It was suggested that possible reasons may be both the closeness of the composition to relaxors with a spontaneous phase transition, in which these temperatures coincide, and large sizes of the polar regions. The field-temperature phase diagram was constructed for cooling the sample in an electric field (FC mode). In the study of time dependences of permittivity in an electric field at room temperature, it was found for the first time that the monoclinic phase after a short time interval of ~ 300 s in high electric fields is transformed into another ferroelectric tetragonal phase. This phase is not stable after the electric field is removed, and the sample returns to its original state before the field was applied.

Keywords: Key words: ceramics, relaxors, ferroelectricity, phase diagram, induced phase transition.

DOI: 10.61011/PSS.2025.02.60683.23-25

1. Introduction

High-temperature piezoelectric materials are widely used in the aerospace industry, nuclear power industry, oil and geothermal well drilling, and in some other devices. Piezoelectric materials, when used in practice, are expected to withstand high temperatures and voltages, which will significantly influence ceramics properties. Many of these applications require an operating temperature higher than 300 °C. Several materials are possible candidates for utilization at high temperatures. Lithium niobate ($LiNbO_3$) has a high Curie temperature (T_C), but its piezoelectric coefficient (d_{33}) is very low [1]. Lead zirconate-titanate (PZT) is another most promising candidate, however, its $T_C \sim 620$ K is quite low and, moreover, it demonstrates high dielectric loss [2]. $Pb(Zn_{1/3}Nb_{2/3})O_3-PbTiO_3$ (PZN−PT) and $Pb(Mg_{1/3}Nb_{2/3})O_3-PbTiO_3$ (PMN−PT) solid solutions are outstanding piezoelectric materials, however, their structural phase transition temperatures are in the range of relatively low temperatures, about 350−400 K [3–6].

$BiFeO_3$ is a well known single-phase multiferroic that has a good piezoelectric response and very high T_C. However, there are many issues with $BiFeO_3$ synthesis giving rise to the formation of defects and additional phases that significantly affect its conductivity [7,8].

$(1-x)BiScO_3 - xPbTiO_3$ (BS−xPT) perovskite-structure ceramic solid solutions with compositions close to a morphotropic phase boundary (MPB) between the rhombohedral and tetragonal phases ($x = 0.64$) feature high piezoelectric constants ($d_{33} \sim 400$ pC/N) compared with PZT that is widely used in piezoceramics [9–11]. However, the Curie temperature of the BS−xPT ceramics($T_C \sim 720$ K) is higher than T_C of PZT by ~ 100 K, thus, allowing the application temperature range to be increased. Therefore, the BS−xPT system has been of high interest to researchers in the recent decade.

Similarly to binary systems, ternary systems have a wider phase boundary and better properties. As a consequence, extensive studies are carried out to investigate the effect of addition of various atoms and components on the electrophysical properties of the BS−xPT ceramics. Such studies are interesting not only from a scientific standpoint, i. e. with more detailed study of high piezoelectric activity mechanisms in the BS−xPT system, but also from a practical standpoint, because they allow to find new promising piezoceramic materials.

Creation of multicomponent systems is the most effective way to combine the advantages of various binary systems, in particular, the highest piezoelectric response of relaxor−PT systems and high Curie temperatures of the BS−xPT system. PT solid solutions with PMN type ferroelectric relaxors (FE-R) shows particularly high piezoelectric properties near MPB. It is known from the literature data [12–15] that some ternary solid solution compositions $(1-2x)BiScO_3 - xPbTiO_3 - xPbMg_{1/3}Nb_{2/3}O_3$ (BS−xPT−xPMN) have high piezoelectric properties. Maximum values $d_{33} \sim 509$ pC/N were found in the studied solid solutions near MPB with $x = 0.42$ [13,14]. Enhancement of the piezoelectric response of these solid solutions may be caused by external contributions (increase in the number of domain configurations, minimized domain structure, etc.) as well as by intrinsic contributions (polarization rotation, proximity of an expected tricritical point, etc.). As a result, the solid solution of interest has a higher d_{33} than that of the BS$-x$PT ceramics, but has a lower Curie temperature ($T_C \sim 425$ K). Thus, it follows that solid solutions with $x = 0.42$ may be used effectively in piezoelectric devices operating at room temperatures.

MPB between the tetragonal and rhombohedral phases in BS$-x$PT$-x$PMN is observed at $x = 0.4-0.42$. Addition of the PMN relaxor changes the properties of BS$-x$PT considerably. In the BS$-x$PT compounds, the maximum dielectric permittivity is not shifted with the frequency, which suggests that they are not relaxors [16]. In the BS$-x$PT$-x$PMN compounds at the MPT (transition) temperature, the polarized sample, when heated, switches from a rhombohedral (a monoclinic phase according to some data) ferroelectric phase to a relaxor tetragonal phase, and then from a tetragonal phase to a cubic phase.

Works devoted to these ternary systems don't contain any information about the relationship between the depolarization temperature of pre-polarized samples T_d and the temperature of ferroelectric-relaxor phase transition $T_{\text{F-R}}$. As is known from the literature and our works [17–23], these temperatures may coincide with each other in a number of relaxors such as PZT, PMN, and may differ, for example, in relaxors such as PZN, PZN$-$PT solid solutions, $Na_{1/2}Bi_{1/2}TiO_3$ (NBT), NBT solid solutions with $BaTiO_3$ (NBT$-$BT) and $(K_{0.5}Na_{0.5})NbO_3-0.02Ba_2NaNb_5O_{15}$ (KNN$-$BNN).

There is no single point of view on the observed difference between T_d and $T_{\text{F-R}}$ in some relaxors. According to some authors [18], depolarization takes place in two stages. At the first stage, heating of the polarized sample to a temperature above T_d destroys only the macroscopic polarization, but the relationship of local dipoles within domains is not lost. With further heating at $T_{\text{F-R}}$, domains are disintegrated into polar nanoregions (PNR). Authors of another work [21] explain the loss of polarization at lower T_d than the long-range order disintegration at $T_{\text{F-R}}$ by the existence of depolarizing fields and voltages due to different deformation at grain boundaries. The study of PMN$-x$PT, PZN$-x$PT, NBT$-x$BT, KNN$-$BNN single-crystal solid solutions in [20,22] suggested that the relative position of the depolarization temperature and the temperature of polarized sample transition to a relaxor phase did not depend on the type of phase boundary (polymorphic or morphotropic), but was associated only with the degree of phase transition smearing and polar region sizes.

Such investigations were not carried out on BS$-x$PT$-x$PMN compounds. The available information on dielectric and piezoelectric properties of these compounds is generally very limited, regardless of the fact that PMN-based solid solutions are the key materials for various applications. Moreover, when such miscellaneous phases are combined (PMN — cubic phase with polar nanoregions, PT — tetragonal phase, BS — centrosymmetric monoclinic phase), a wide variety of ternary system properties may be expected. Interest in these investigations is also associated with the fact that the predominant composition of BS$-x$PT is not a relaxor, and the phase boundary is a mixture of two boundaries: MPB below 300 °C and polymorphous boundary above 300 °C [24,25]. This means that the polymorphic phase boundary (PPB) is not vertical in the temperature–composition phase diagram and shows a strong temperature dependence, while MPB is vertical. MPB curvature may affect the applicable temperature range.

The objective of this work was to study the correlation between T_d and $T_{\text{F-R}}$ in the 16BS$-$42PT$-$42PMN (BS$-$42PT$-$42PMN) relaxor ceramics, and polar nanoregion (PNR) development kinetics in ferroelectric phase induction. Moreover, the study will examine how the phase stability of intermediate phases varies (in particular, of a tetragonal phase), when the sample is cooled in an electric field. Study of the relative position of T_d and $T_{\text{F-R}}$ in this ceramics is of particular interest because this is the first study of this kind among the already-studied ferroelectrics [17–22], where the predominant compound is not a relaxor [9–11]. For most of applications, T_d is an important parameter because piezoelectric and pyroelectric effects depend to a lesser degree on the long-range order between local dipoles and to a greater degree on the capability to maintain macroscopic residual polarization.

2. Examined samples and experimental procedure

BS$-$42PT$-$42PMN ceramic samples were prepared using a common ceramic technique [12–14]. Pellets, 10 mm in diameter and 0.5 mm in thickness, were made from sintered ceramic blanks by cutting and grinding. Polarization of the samples was performed at 380 K in $2-40$ kV/cm electric fields during 30 min. Then, the sample was cooled to room temperature in the same field. MPT in these compounds is observed at $\sim 340-350$ K.

Dielectric measurements without/with an electric field were carried out at a frequency of 1 kHz in the temperature range of $290-500$ K. Permittivity ε and $\tan\delta$ were measured in two electric field modes: 1) Measurement of ε with zero-field heating after field cooling of the sample (ZFHaFC). Field was applied at a temperature higher than maximum ε; 2) Measurement of ε with cooling of the sample in fields with different strength (FC mode). Dependences of relative permittivity $(\varepsilon/\varepsilon_0)$ on time were studied using the E7-15 LCR meter in $0-20$ kV/cm electric fields at room temperature below the Vogel–Fulcher temperature. Before each measurement, the samples were annealed during 15 min at a temperature 50 K as high as the maximum permittivity temperature to avoid memory effects in the samples that are induced by the applied electric field. After annealing, the samples were zero-field cooled to room temperature, at which constant electric fields with different strengths were applied to them. After the electric field application, permittivity variation with time was recorded. The measurements were carried out directly after annealing of the samples.

Thermally stimulated depolarization (TSD) or pyrocurrent was studied according to the following scheme: the sample was zero-field pre-heated to 400 K (ZFH), then cooled in the temperature range from 400 K to 173 K at a rate of 5 K/min in the 20 kV/cm external filed (FC). Then, the field was switched off and the sample was held in the short-circuited state for 15 min. Then the sample was zero-field heated in the temperature range 173–400 K at a constant rate of 5 K/min (ZFHaFC mode) and the depolarization current was measured. The procedure was fully repeated for the other electric field polarity. Polarization was calculated by integrating the TSD current density with time. Heating and cooling were performed in dry nitrogen atmosphere with computer-controlled temperature conditions with accuracy of 0.2 K according to a pre-set program. FC polarization of the sample in a field up to 20 kV was provided by a PS-350/5000V high-voltage source. TSD current was measured in the ZFHaFC mode using the U5-11 electrometer amplifier with analog-to-digital converter, sensitivity 10^{-15} A.

3. Experimental results and discussion

Figure 1 shows the temperature dependences of ε (curves *1, 1'*) and $\tan\delta$ (curves *2, 2'*) in the BS–42PT–42PMN samples obtained during zero-field heating and cooling. Besides the major maximum corresponding to a transition to a cubic phase, no additional anomalies were found on ε curves at the MPT temperature. There are no any significant anomalies on $\tan\delta$ curves either in transition to a cubic phase or at the MPT temperature. Note that shift of the permittivity maximum is not observed within the measurement error during heating and cooling of the sample (curves *1* and *1'*). This data agrees with the data in [13,14] obtained for samples with the same composition. The absence of dielectric hysteresis is a common feature of second-order phase transitions.

As it follows from [13,14], increase in the content of PMN to values higher than $x = 42$ gives rise to significant temperature hysteresis that is typical of the first-order phase transition. Transformation of properties from a relaxor ferroelectric state to a normal ferroelectric state is observed in compounds with $x > 0.42$. In [13,14], an assumption is put forward regarding the existence of tricritical point on the phase diagram in BS–xPT–xPMN compounds near $x = 0.42$.

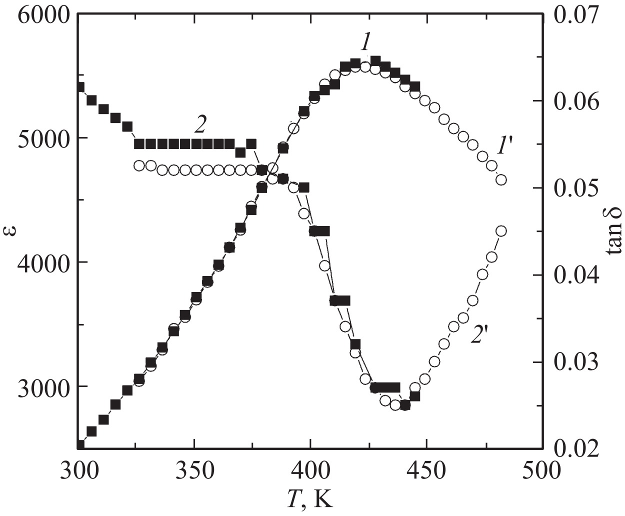

Figure 1. Temperature dependences of ε (*1, 1'*) and $\tan\delta$ (*2, 2'*) in BS–42PT–42PMN samples obtained in heating (*1, 2*) and cooling (*1', 2'*).

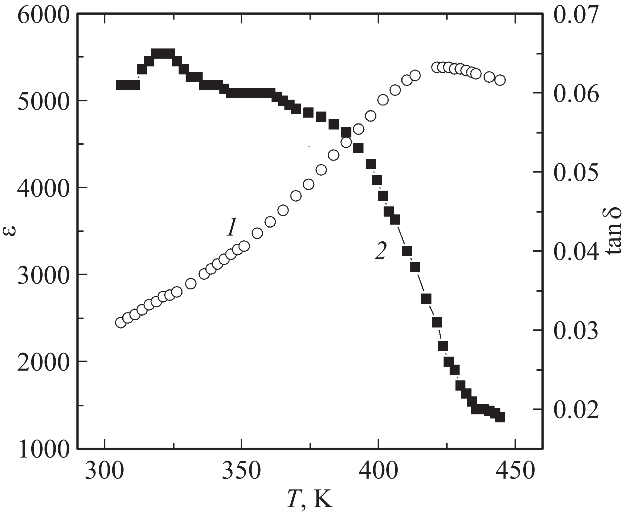

Figure 2. Temperature dependences of ε (*1*) and $\tan\delta$ (*2*) measured in zero-field heating after polarization in the 22 kV/cm field (ZFHaFC mode).

Figure 2 shows the temperature dependences of ε (curve *1*) and $\tan\delta$ (curve *2*) measured in the ZFHaFC mode after polarization in the 22 kV/cm field. No significant changes were found on ε curve, besides the maximum corresponding to a transition to a cubic phase. Temperature dependence of $\tan\delta$ (curve *2*) shows insignificant anomalies: a small maximum at 318–320 K and a plateau at 340–350 K, after which sharp decrease in $\tan\delta$ starts. Similar anomalies on $\tan\delta$ curve were observed after polarization of the sample also in other fields.

Previously in [12], the temperature dependence of $\tan\delta$ measured in heating of samples with $x = 0.42$ in the 2 kV/cm field showed also two anomalies at 318 K and 345 K. The authors explained that the observed anomalies were caused by the field-induced ferroelectric relaxor-ferroelectric phase transition (318 K) and by a reverse ferroelectric — ferroelectric relaxor transition (345 K), respectively. At the same time, during heating of a polarized sample (ZFHaFC mode), the authors observed only one anomaly on $\tan\delta$ curve at 345 K corresponding to a transition to a ferroelectric relaxor state.

Two anomalies were observed in this work at the same temperatures during zero-field heating of a polarized sample (Figure 2). It was assumed that a small maximum of $\tan\delta$ at 318−320 K corresponded to the sample depolarization temperature T_d, and the change of the curve slope corresponded to $T_{\mathrm{F-R}}$ at 340−350 K. Two perovskite phases: major and additional C-phases, are observed at room temperature in sample $x = 0.42$ according to the X-ray diffraction analysis performed in [13,14,16]. The major phase consists of a monoclinic and tetragonal phase mixture. After electric field application, the induced ferroelectric state and macroscopic polarization (partial or full, depending on the applied field) are destroyed at temperatures above T_d, but the interconnection of local dipoles within domains is not lost. Only after the MPT temperature (~ 350 K), polar nanoregions appear, long-range order is completely destroyed, and the sample changes into the relaxor phase [12]. Thus, $T_{\mathrm{F-R}}$ is the upper depolarization boundary.

To verify this assumption, temperature dependences of pyrocurrent and polarization were measured. These measurements are shown in Figure 3, *a* and *b*.

As shown in Figure 3, *a*, the pyrocurrent maximum is observed at $\sim 345{-}348$ K, which almost coincides with $T_{\mathrm{F-R}}$, rather than with the temperature of the observed $\tan\delta$ maximum (318 K) (Figure 2). Thus, our assumption that $\tan\delta$ maximum corresponds to T_d doesn't prove true, because T_d is actually the temperature at which the pyroelectric current maximum is observed, which corresponds to the inflection point of the residual polarization curve [26]. Pyrocurrent anomaly at $T_{\mathrm{F-R}}$ was observed in samples with the same composition and in [12]. The conducted measurements suggest that these temperatures coincide with each other, i. e. the ferroelectric-relaxor transition is a single-step process.

Note that the temperature dependences of pyrocurrent and thermally stimulated depolarization are highly smeared (Figure 3) compared, for example, with other relaxor compositions such as PLZT, NBT−PT [26]. Depolarization starts much earlier than the depolarization temperature is reached ($T_d = T_{\mathrm{F-R}} = 345{-}348$ K), and the degree of depolarization is much lower than, for example, in PLZT, NBT−BT.

When comparing the pyrocurrent behavior (Figure 3, *a*) with findings published in [12] for the same composition $(1-2x)$BS−xPT−xPMN ($x = 0.42$), then the temperatures of the measured maxima coincide and are equal to ~ 345 K, despite some difference in the sample polarization conditions and pyrocurrent measurement. Differences display themselves in the height of $J_{\max+} = 24$ and $J_{\max-} = -28\,\mathrm{nA/cm^2}$, which corresponds to $p_{\max+} = 289$ and $p_{max-} = -336\,\mathrm{nC/(cm^2\cdot K)}$ with reference to the accepted pyrocurrent values $p_{\max+} = 289$ and $p_{max-} = -336\,\mathrm{nC/(cm^2\cdot K)}$. These values are approximately twice as low as $p_{\max 1} \sim 450\,\mathrm{pC/(cm^2\cdot K)}$ and $p_{\max 2} \sim 650\,\mathrm{pC/(cm^2\cdot K)}$ obtained in [12] on samples polarized at room temperature and 500 K, respectively. The smeared maximum (Figure 3, *a*) is evaluated by $\Delta T(p_{1/2\,\max}) = 50$ K, which is a little lower than more smeared maxima in [12], whose $\Delta T(p_{1/2\,\max}) \sim 80$ K.

There are several potential reasons for the smeared pyrocurrent maximum and gradual decrease in depolarization in ceramics studied in this work. One of the reasons may be in the mixed phase structure and co-existence of miscellaneous polar domains. Applied electric field induced partial monodomainization of the sample and ferroelectric long-range order only in a part of the sample volume and, consequently, to the co-existence of ferroelectric rhombohedral (or monoclinic) phase domains and tetragonal relaxor phase domains in a wide temperature range. These domains with different symmetry are arranged differently in external fields and have different transition temperatures. At $T_{\mathrm{F-R}}$, the major part of the sample changes to the relaxor phase, but a minor part of ferroelectric domains with spontaneous polarization remains. As the temperature grows, the number of ferroelectric domains decreases and depolarization gradually disappears.

The second reason may be in the ageing effect. Study of the lead-containing relaxor PMN−12PT in [27] found that smearing of the pyrocurrent maximum increases with the ageing time. Regardless of the fact that the samples studied in this work were annealed before measurements, ageing during cooling and measurement cannot be completely avoided. Identical depolarization behavior and smeared pyrocurrent maximum in a wide temperature range were observed previously in BNT−BT−KNN [28] and PMN−0.06PT [29] materials. Ageing behavior in various compounds shall be investigated to identify its influence on the depolarization behavior.

Space charge effect on the polarization temperature behavior also cannot be avoided in our ceramics (Figure 3, *b*) and is slightly different from the classical dependence $P(T)$ for simulated ferroelectrics. The space charge effect on ceramics polarization is more substantial than in the single-crystal sample case and may be associated not only with charge carrier traps on crystal structure irregularities, but also with charge distribution at ceramics grain boundaries [30]. In Figure 3, *b*, the ferroelectric residual polarization curve is probably located against the background of polarization associated with the frozen space charge. In this case, background current of $10\,\mathrm{nA/cm^2}$ caused by thermally stimulated space-charge depolarization is observed at a low temperature region below 250 K. Note that in [12] TSD current maxima without any visible background were obtained after polarization of samples either at room temperature or in FC mode in the temperature range 500−300 K. In this work, filed cooling was carried out in the temperature range from 400 K to 173 K. During measurement in this temperature range, polarization process may also take place together with the ferroelectric polarization process due to spatial redistribution of the space

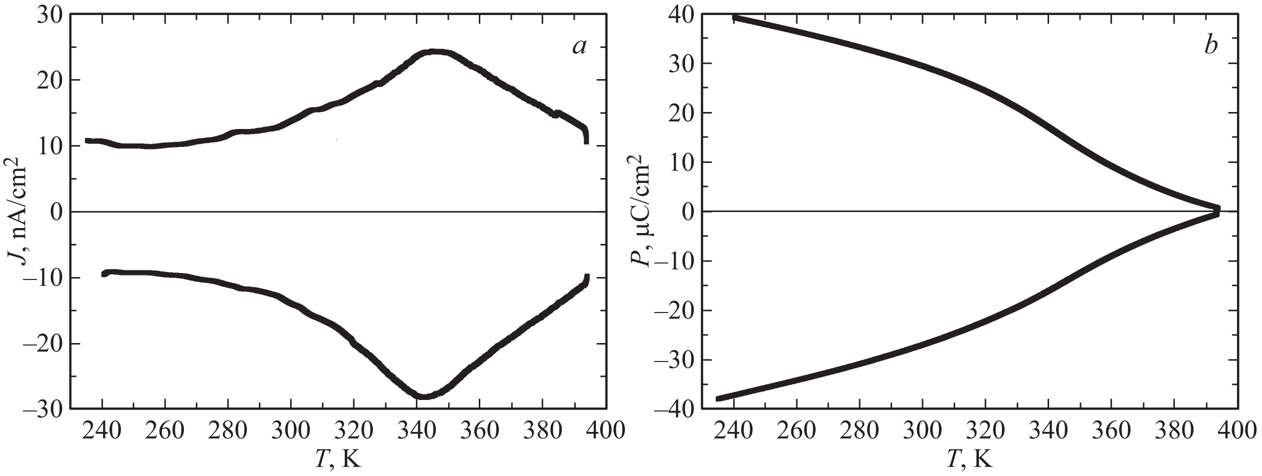

Figure 3. Temperature dependences of thermally stimulated depolarization current (pyrocurrent) density after cooling of the sample in the 20 kV/cm field (a) and polarization as a result of TSD current (pyrocurrent) integration (b). Temperature region of residual polarization is lower than 345−348 K.

charge in the external field and may be frozen at low temperatures.

Let's consider the potential causes of coincidence of $T_{\mathrm{F-R}}$ and T_d in the studied BS−42PT−42PMN ceramics. One of the potential causes is associated with the composition of the studied ceramics. Normal BS−xPT ferroelectric (not relaxor) is a predominant component, and $T_{\mathrm{F-R}}$ and T_d coincide in the PMN relaxor compound [23].

Another potential cause is the fact that the compound with $x = 0.42$ is at the boundary between the normal ferroelectric and relaxor. As it follows from [13,14], the potential barrier E_a in the Vogel–Fulcher in the $(1-2x)$BS−xPT−xPMN compound for $x \leq 0.38$ ($E_a \sim 0.045$ eV) is comparable with that for PMN compounds where the relaxor state is stable ($E_a \sim 0.071$ eV for PMN). For compounds with $x > 0.38$, quick decrease in E_a is observed (for $x = 0.42$ $E_a \sim 0.033$ eV, for $x = 0.46$ $E_a \sim 0.012$ eV) to values typical of relaxors with a spontaneous phase transition to a ferroelectric state such as $\mathrm{PbSc_{1/2}Ta_{1/2}O_3}$ (PST) ($E_a \sim 0.023$ eV) and $\mathrm{PbSc_{1/2}Nb_{1/2}O_3}$ (PSN) ($E_a \sim 0.014$ eV). This fact also indicates that there is a relaxor-ferroelectric transition, if $x > 0.42$. Actually, it is shown in [13,14] that, as x grows in these compounds, growth of coercive field (E_c), maximum polarization (P_m) and residual polarization (P_{rem}) is observed, and a maximum is observed on the concentration dependences of the last two parameters near MPB at $x \sim 0.42$. Growth of E_c, P_m and P_{rem} is probably induced by formation of macroscopic domain structures in transition to the normal ferroelectric state and by a stronger effect of domain orientation processes on polarization. Maxima of P_m and P_{rem} on its concentration dependences near MPB may be associated with co-existence of ferroelectric phases.

In such compounds, the number and concentration of polar regions are insignificant at the Curie temperature and, as the temperature decreases, PNR sizes can increase considerably up to macroscopic ferroelectric domains. In [31–33], it was shown that the Vogel–Fulcher temperature T_{F} in the compositionally disordered PST and PSN crystals almost coincided both with the temperature of a maximum on the temperature dependence of static susceptibility (T_A is close to $T_{\max}$) and the spontaneous phase transition temperature T_{C} and, therefore, with the depolarization temperature.

The authors of [34] used a scanning electron microscope to measure a mean grain size in the BS−PT−xPMN ($x = 0.34{-}0.42$) ceramics at MPB and to determine the relation between the grain size and x. Grain sizes turned to be rather big and varied from 10.2 mkm to 5.1 mkm as x decreased. Apart from the grains size, the fraction of larger grains increased as the content of PT increased. It is well known that the domain size in ferroelectric materials is closely related to the corresponding grain size.

Origin of the maximum on the temperature dependence of $\tan\delta$ at 318 K, when polarized samples are heated, requires further investigations.

To clarify the stability of intermediate phases (in particular, tetragonal phase) and its evolution depending on the electric field strength, dielectric properties were measured in the FC mode in constant electric fields with different strength. As an example, Figure 4 shows temperature dependences of $\tan\delta$ (curves *1, 2*) and ε (inset in Figure 4) in the sample cooled in fields with different strength. The inset in Figure 4 shows the maximum position of permittivity vs. temperature. A small maximum of $\tan\delta$ is observed at the MPT temperature. It can be seen from Figure 4 that the maximum position of permittivity as well as $\tan\delta$ at the MPT temperature within the measurement error doesn't depend on the field strength. Similar dependences were also observed in other fields.

Using the dielectric measurement data in different electric fields (Figure 4), a field–temperature phase diagram was built for the FC mode as shown in Figure 5. Two phase

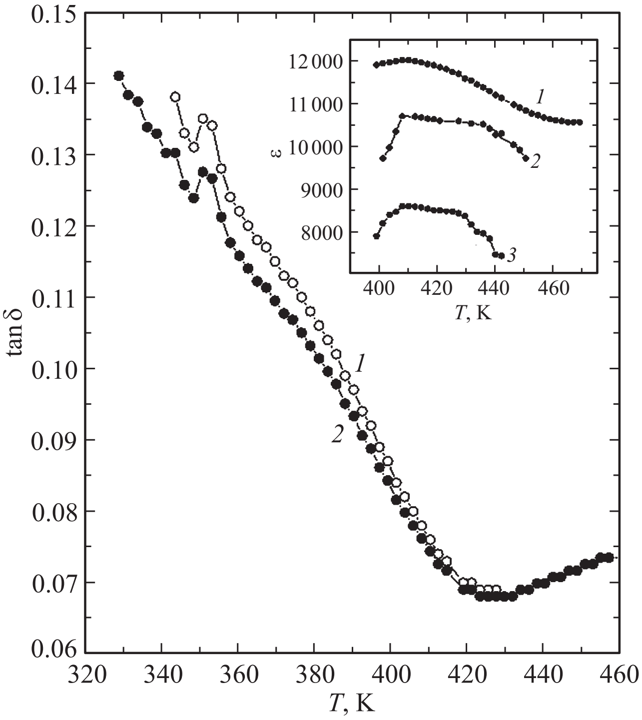

Figure 4. Temperature dependences of $\tan\delta$ in the BS$-$42PT$-$42PMN sample measured in the FC mode in different electric fields E, kV/cm: *1* — 2, *2* — 10. Inset — permittivity maximum position in the FC mode in different fields, kV/cm: *1* — 0, *2* — 2, *3* — 10.

transitions are induced during field cooling. Figure 5 shows that the phase boundary between the cubic and tetragonal phases and between the tetragonal and monoclinic phases (MPT) is almost a vertical line, i. e. its position almost doesn't depend on the applied field strength.

The absence of any significant sift between the cubic and ferroelectric phases may be due to a small fraction of relaxor phase where the cubic and ferroelectric phases coexist. Compound with $x = 42$ is exactly on the boundary between the ferroelectric relaxor and normal ferroelectric. A major part of the volume is taken by the ferroelectric phase whose elastic energy density is much higher than that of the relaxor phase, which may result in that it will be difficult for the electric field to move the phase boundary. An almost vertical segment is observed in transition between the tetragonal and monoclinic phases (MPT). In [22,23], reasons for the occurrence of such quasi vertical line during field cooling of PMN$-x$PT ($6 < x < 30\%$) solid solutions were discussed. Position of this line is close to the Vogel–Fulcher temperature, and solid solution properties above and below this temperature differ considerably. For example, at this temperature, the polarized sample is depolarized in zero field, frequency dispersion of ε in the FC process stops, which indicates that polar nanoregions get „frozen" and the regions themselves grow in size. This line most likely means that a macroscopic metastable state occurs due to freezing of large polar regions [24]. The ferroelectric phase is nonstable above this line and is metastable below this line and may be formed above some threshold electric field value.

Figure 6 (curves *1, 2*) shows time dependences of permittivity variations $(\varepsilon/\varepsilon_0)$ at room temperature in different electric fields 6 kV/cm (curve *1*) and 14 kV/cm (curve *2*), where ε_0 is the permittivity before field application, ε is

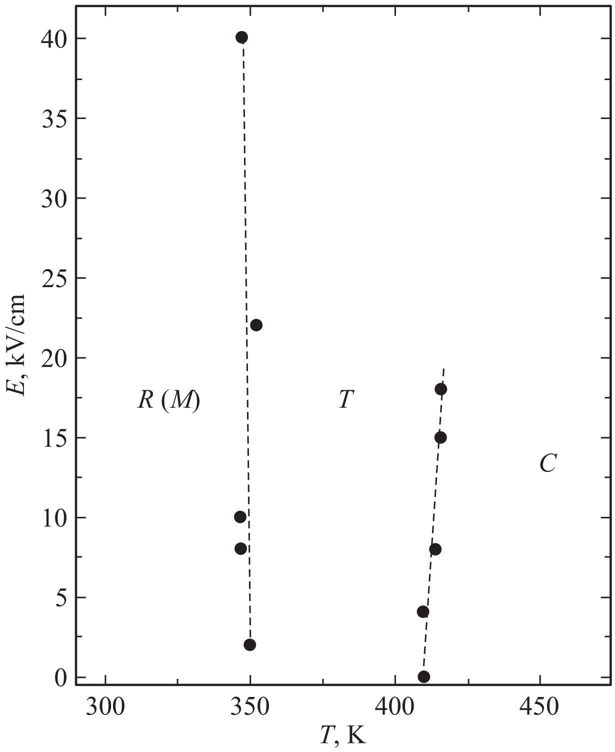

Figure 5. $E-T$ phase diagram for BS$-$42PT$-$42PMN crystals obtained in the FC mode.

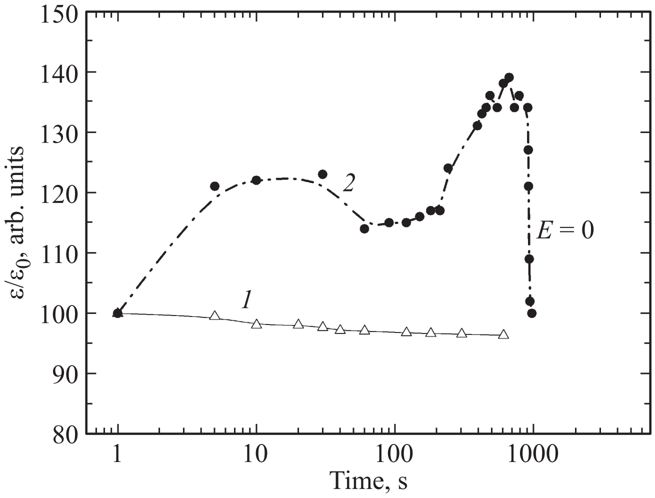

Figure 6. Relative variations of permittivity $\varepsilon/\varepsilon_0$ (ε_0 — permittivity in zero-field) with time in the 16BS$-$42PMN$-$42PT ceramics in different electric fields applied at room temperature, E, kV/cm: *1* — 6, *2* — 14. After 1000 s, electric field was switched off.

the permittivity in different times. Field was applied to the sample during 1000 s and then switched off. It can be seen that almost no changes of $\varepsilon/\varepsilon_0$ are observed in the fields much weaker than the coercive field (curve *1*) ($E_c = 9$ kV/cm [13,14]), In fields stronger than the coercive field (curve *2*), variation of $\varepsilon/\varepsilon_0$ occurs immediately after field application. A small maximum is observed at short times after field application. Occurrence of the maximum after field application may be associated with the activation of monoclinic domains switch-over processes, which are observed at $E > E_c$, as well as with an increase in the mobility of domain walls during the sample polarization. Decrease in $\varepsilon/\varepsilon_0$ downstream of the maximum indicates that the sample is partially monodomainized and the monoclinic phase occurs in a part of the sample volume. Then, after a short time period an increase in $\varepsilon/\varepsilon_0$ was detected that was probably due to the induced phase transition from monoclinic to tetragonal phase. The resultant tetragonal phase is not stable any longer after removal of the electric field, which is indicated by a sharp decrease in $\varepsilon/\varepsilon_0$ to the initial value of ε_0.

Results shown in Figure 6 agree well with our data obtained in [35] regarding the dependences of the longitudinal deformation S of the studied ceramics on the electric field. In fields close to a coercive field, fast growth of S was observed on the dependence $S = f(E)$ due to the contribution of domain switching activated near coercive electric fields and to partial monodomainization of the sample (within a grain). With further increase in the field to $E = 14$ kV/cm, hysteresis between the direct and reverse dependence $S{-}E$ disappeared and a strongly pronounced inflection was observed, which may be associated with a monoclinic-tetragonal transition induced by a strong electric field. Existence of the field-induced transition to a tetragonal phase is also supported by the X-ray diffraction examination of the solid solution sample of interest [36].

The MPT to tetragonal phase in the ceramics with this composition takes place in the temperature range of 345−350 K. Room temperature, at which time measurements were conducted, was quite close to the MPT temperature, therefore even at this temperature a transition to a tetragonal phase was observed in strong electric fields and after a small time period.

The absence of delay time during induction of a ferroelectric phase observed in the 16BS−42PMN−42PT ceramics may occur most likely due to the growth of polar region sizes (PNR).

4. Conclusion

This work investigated the relation between T_d (depolarization temperature) and $T_{\mathrm{F-R}}$ (morphotropic phase transition temperature) in the polarized 16BS−42PT−42PMN relaxor ceramics, and the polar nanoregion (PNR) development kinetics during ferroelectric phase induction.

Coincidence of these temperatures was found due to a single-stage transition of the polarized sample to a relaxor phase. Compound with $x = 0.42$ is at the boundary between a normal ferroelectric and relaxor, and has a potential barrier comparable with relaxors that have spontaneous phase transitions. In such compounds, the number and concentration of polar regions are insignificant at the Curie temperature and, as the temperature decreases, PNR sizes can increase considerably up to macroscopic ferroelectric domains. In this case, the Vogel–Fulcher temperature T_{F} almost coincides with the depolarization temperature. Composition of the ceramics of interest is another possible cause of the temperature coincidence. Normal ferroelectric (not relaxor) is a predominant component, and $T_{\mathrm{F-R}}$ and T_d coincide in the additional PMN component.

A field–temperature phase diagram was built for the FC field application mode.

Kinetics of formation of ordered ferroelectric phases in different electric fields applied below the MPT temperature. It was found that, immediately after application of a field exceeding a coercive field, increase in $(\varepsilon/\varepsilon_0)$ is initially observed on the time dependences of permittivity $(\varepsilon/\varepsilon_0)$ and a small smeared maximum occurs with time. This maximum may be associated with the activation of monoclinic domain switch-over processes, which are observed at $E > E_c$, as well as with an increase in the mobility of domain walls during the sample polarization, and with partial monodomainization of the sample to a monoclinic phase. After a short time ~ 300 s, further increase in $\varepsilon/\varepsilon_0$ was first found in strong electric fields in this ceramics, which may be attributable to the transformation of this monoclinic phase into another ferroelectric tetragonal phase. This phase is not stable any longer after removal of the electric field, and the sample returns to its initial state before the field application.

Conflict of interest

The authors declare that they have no conflict of interest.

References

[1] R. Weis, T. Gaylord. Appl. Phys. A **37**, 191 (1985).
[2] S.E. Park, T.R. Shrout. J. Appl. Phys. **82**, 1804 (1997).
[3] E. Sun, W. Cao. Prog. Mater. Sci. **65**, 124 (2014).
[4] S. Zhang, F. Li, X. Jiang, J. Kim, J. Luo, X. Geng. Prog. Mater Sci. **68**, 1 (2015).
[5] S. Zhang, F. Li. J. Appl. Phys. **111**, 031301 (2012).
[6] K. Uchino. Piezoelectric actuators and ultrasonic motors. Boston Kluwer (1997). 350 p.
[7] F. Mumtaz, G.H. Jaffari, Q. Hassan, S.I. Shah. Physica B: Condensed Matter **538**, 213 (2018).
[8] L. Soibam, A.D. Mani. Mater. Today **5**, 2064 (2018).
[9] J. Wu, H. Shi, T. Zhao, Y. Yu, S. Dong. Adv. Funct. Mater. **26**, 7186 (2016).
[10] J. Chen, G. Liu, J. Cheng, S. Dong. Appl. Phys. Lett. **107**, 032906 (2015).

[11] J. Chen, J. Cheng, S. Dong. J. Adv. Dielectr. **4**, 1430002 (2014).

[12] A.A. Bush, K.E. Kamentsev, M.A. Bekhtin, A.G. Segalla. FTT **59**, 36 (2017) (in Russian).

[13] M.V. Talanov, A.A. Bush, K.E. Kamentsev, V.P. Sirotinkin, A.G. Segalla. J. Am. Ceram. Soc. **101**, 683 (2018).

[14] M.V. Talanov, A.A. Bush, K.E. Kamentsev, V.P. Sirotinkin, A.G. Segalla. Ferroelectrics **538**, 105 (2019).

[15] C.J. Stringer, N.J. Donnelly, T.R. Shrout, C.A. Randall, E.F. Alberta, W.S. Hackenberger. J. Amer. Ceram. Soc. **91**, 1781 (2008).

[16] K. Shahzad, L. Li, Z. Li, G. Shabbir, H. Li, X. Yao. Ferroelectrics **402**, 142 (2010).

[17] A.I. Spitsin, A.A. Bush,K.E. Kamentsev, V.P. Sirotinkin, M.V. Talanov. Tonkie khimicheskie tekhnologii, **14** (79), (2019) (in Russian).

[18] E. Sapper, S. Schaab, W. Jo, T. Granzow, J. Rödel. J. Appl. Phys. **111**, 014105 (2012).

[19] Y. Hiruma, H. Nagata, T. Takenaka. J. Appl. Phys. **105**, 084112 (2009).

[20] L.S. Kamzina. FTT **64**, 665 (2022). (in Russian).

[21] A.B. Kounga, T. Granzow, E. Aulbach, M. Hinterstein, J. Rödel. J. Appl. Phys. **104**, 024116 (2008).

[22] L.S. Kamzina. FTT **66**, 579 (2024). (in Russian).

[23] V. Bobnar, Z. Kutnjak, R. Pirc, A. Levstik. Phys. Rev. B **60**, 6420 (1999).

[24] R.E. Eitel, S.J. Zhang, T.R. Shrout, C.A. Randall, I. Levin. J. Appl. Phys. **96**, 2828 (2004).

[25] J. Chaigneau, J.M. Kiat, C. Malibert, C. Bogicevic. Phys. Rev. B **76**, 0941111 (2007).

[26] W. Jo, R. Dittmer, M. Acosta, J. Zang, C. Groh, Eva Sapper, K. Wang, J. Rödel. J. Electroceram. **29**, 71 (2012).

[27] E.V. Colla, D. Vigil, J. Timmerwilke, M.B. Weissman, D.D. Viehland, B. Dkhil. Phys. Rev. B **75**, 214201 (2007).

[28] X. Tan, E. Aulbach, W. Jo, T. Granzow, J. Kling, M. Marsilius, H.J. Kleebe, J. Rödel. J. Appl. Phys. **106**, 044107 (2009).

[29] E.V. Colla, M.B. Weissman. Phys. Rev. B **72**, 104106 (2005).

[30] K. Okadzaki. Tekhnologiya keramicheskikh dielektrikov. Energiya, M. (1976). 336 s. (in Russian).

[31] F. Chu, N. Setter, A.K. Tagantsev. J. Appl. Phys. **74**, 5129 (1993).

[32] F. Chu, I.M. Reaney, N. Setter. Ferroelectrics **151**, 343 (1994).

[33] F. Chu, I.M. Reaney, N. Setter. J. Appl. Phys. **77**, 1671 (1995).

[34] G. Xie. Symposium on Piezoelectricity, Acoustic Waves, and Device Applications, Oct. 27–30, Chengdu, Sichuan, China, 537 (2017).

[35] L.S. Kamzina, M.V. Talanov, A.A. Bush, A.I. Spitsin. FTT **61**, *8*, 1483 (2019) (in Russian).

[36] A.A. Bush, V.G. Sirotinkin, A.G. Segallo, A.I. Spitsin. Kristallografiya **63**, 93 (2018) (in Russian).

Translated by E.Ilinskaya